Research Square

Preprints are preliminary reports that have not undergone peer review.
They should not be considered conclusive, used to inform clinical practice,
or referenced by the media as validated information.

Nonlinear temperature-dependent thermal conductivity estimation based on Kirchhoff transformation

Sidney Ribeiro

sidney.silveira@ufu.br

Federal University of Uberlândia

Gilmar Guimarães

Federal University of Uberlândia

Research Article

Keywords: Inverse problem, IHCP, Kirchhoff transformation, Nonlinear heat problem, Temperature-dependent thermal conductivity

Posted Date: June 8th, 2026

DOI: https://doi.org/10.21203/rs.3.rs-9814840/v1

License: This work is licensed under a Creative Commons Attribution 4.0 International License.
Read Full License

Additional Declarations: No competing interests reported.

Nonlinear temperature-dependent thermal conductivity estimation based on Kirchhoff transformation

Sidney Ribeiro[1*] and Gilmar Guimarães[1*]

[1*]Department of Mechanical Engineering, Federal University of Uberlândia, João Naves de Ávila Avenue, 2121, Uberlândia, 38408-109, Minas Gerais, Brazil.

*Corresponding author(s). E-mail(s): sidney.silveira@ufu.br; gguima@ufu.br;

Abstract

Understanding temperature-dependent thermal conductivity is crucial for process optimization and material characterization. However, most thermal processes involve variations in thermal properties, meaning these properties depend on temperature. This phenomenon becomes particularly significant in cases involving large temperature gradients. In this context, this paper presents an inverse problem methodology for estimating temperature-dependent thermal conductivity, assuming a polynomial variation. The approach utilizes the direct application of the Kirchhoff transform to experimental data, considering only one accessible surface and determining thermal conductivity profiles based on the temporal evolution of temperature. Essentially, we address the problem of estimating the coefficients of a polynomial model for thermal conductivity. Calculations were performed for different polynomial models, followed by analyses and comparisons with experimental data. The results confirm the accuracy and applicability of the proposed method in this study.

Keywords: Inverse problem, IHCP, Kirchhoff transformation, Nonlinear heat problem, Temperature-dependent thermal conductivity

1 Introduction

Heat transfer process modeling and the accurate determination of thermophysical properties are essential tools for manufacturing and engineering system design. These tools enhance efficiency and optimize operating conditions while reducing the need for costly experimental testing [1]. Thermal conductivity, in particular, is a limiting factor in several applications due to its direct impact on thermal damage to parts, the generation of residual stresses, and the service life of components [1, 2]. Within this context, the global performance of systems such as thermal protection systems (TPS) for hypersonic vehicles [3, 4], thermal energy storage based on phase change materials (PCMs) [5], and machining processes [1] is significantly dependent on this property. Consequently, modeling and predicting operating temperatures have become of great interest, as they allow for a deeper understanding of critical issues regarding structural integrity and thermal distortions [1, 6].

Historically, the development of analytical and numerical models to predict temperatures has been conducted through direct formulations or the Inverse Heat Conduction Problem (IHCP). In early investigations, Yang proposed a linear inverse model combining implicit finite differences and nonlinear optimization to estimate thermal conductivity in one-dimensional problems using temperatures measured inside the solid [7, 8]. Subsequently, Sawaf et al. and Cui et al. advanced inverse analyses using gradient-based algorithms, such as the Levenberg-Marquardt (LM) method and the Conjugate Gradient Method (CGM), to simultaneously estimate multiple temperature-dependent parameters in orthotropic media and ablative composites [6, 9]. Other approaches focused on analytical simplifications, such as the application of the Kirchhoff transformation, to convert the heat conduction problem, highly nonlinear due to variable thermal conductivity, into a linear equation based on apparent temperature [10–12].

More recently, the use of metaheuristic optimization, statistical models, and artificial intelligence has expanded the capacity for thermal prediction in the literature. Farahani and Kisomi, for instance, employed the Heat Transfer Search (HTS) algorithm to identify the conductivity coefficient in solid polymers [13]. Simultaneously, Zhang et al. and Wang et al. proposed transient methodologies using Genetic Algorithms (GA) to characterize the relationship between conductivity and temperature in insulation materials under large thermal gradients [14, 15]. At the forefront of uncertainty quantification, approaches based on Bayesian inference have been successfully implemented to handle measurement noise in stainless steel plates [16]. Additionally, Deep Learning methods, such as Physics-Informed Neural Networks (PINNs) and hybrid architectures (Bi-LSTM-MSA), have been introduced to predict conductivity in a continuous adaptive manner without the need to assume prior functional forms [17, 18].

Despite these advancements, many models still rely on simplifications that treat thermal conductivity as a constant value to facilitate mathematical solutions [1]. However, this temperature dependence can significantly influence predicted temperatures, compromising the accuracy of the evaluations [19, 20]. To circumvent this limitation, recent research has focused on methods that treat thermal conductivity as strictly temperature-dependent. The treatment of this strong nonlinearity is fundamentally

based on the application of mathematical transformations [10, 11, 21], classical inverse techniques combined with global search algorithms [6, 15], and artificial intelligence tools applied to heat transfer [17, 18]. In this scenario, the present work introduces an inverse problem methodology for estimating temperature-dependent thermal conductivity varying polynomially. The approach utilizes the direct application of the Kirchhoff transformation to experimental data, considering only one access surface and determining thermal conductivity profiles based on the temporal evolution of temperature.

2 Theory and Calculation

This section intends to address the inverse problem, which consists of estimating the thermal conductivity for a nonlinear problem, that is, estimating the temperature-dependent thermal conductivity $k(T)$. Starting from the fact that:

$$\Phi = k(T) = \frac{1}{k_0}\int_0^T k(\widehat{T})d\widehat{T}, \tag{1}$$

defines the Kirchhoff transform [22], typically used to linearize nonlinear heat conduction problems where thermal conductivity is a function of temperature, with $k(T) = F(k_0, A_1, A_2, \cdots, A_n, T)$ being a generic function for thermal conductivity. It is observed that F is a function of the reference thermal conductivity k_0, the constants A_n, and the temperature T. Assuming F is continuous, integrable, and its integral has an inverse, then there exists a function $\widehat{F}$ such that:

$$\Phi = k(T) = \frac{1}{k_0}\int_0^T F(k_0, A_1, A_2, \cdots, A_n, \widehat{T})d\widehat{T} = \widehat{F}(k_0, A_1, A_2, \cdots, A_n, T) \tag{2}$$

Since

$$T(x,t) = k^{-1}(\Phi) \tag{3}$$

This directly implies that

$$T(x,t) = \widehat{F}^{-1}(k_0, A_1, A_2, \cdots, A_n, \Phi) \tag{4}$$

Where the function $\Phi(x,t)$ in Eq.(4) represents the temperatures obtained from the linear version of the problem. It can be observed that Eq.(4) establishes a direct relationship between the temperatures of the linear and nonlinear (experimental) versions of the thermal problem as a function of the constants $A_1, A_2, \cdots, A_n$. In this sense, the goal is to determine the coefficients of the function $k(T)$ based on the knowledge of the experimental temperatures of a nonlinear problem and the linear version of the thermal problem, calculated numerically using the same boundary conditions, geometry, and thermal properties. Thus, knowing the terms $T(x,t)$ and $\Phi(x,t)$ from Eq.(4), it remains to determine the coefficients $A_1, A_2, \cdots, A_n$ in polynomial functions of $k(T)$. Considering the specific case $k(T) = k_0(1 + AT)$, where A is a constant:

$$\Phi(x,t) = k(T) = \frac{1}{k_0}\int_0^T k_0(1 + A\widehat{T})d\widehat{T} \Rightarrow \Phi(x,t) = k(T) = \frac{AT^2}{2} + T \tag{5}$$

Note that in Eq.(5), we have $\Phi(x,t) = \frac{AT^2}{2} + T$ where the constant A can be easily isolated, becoming a function of T and Φ. Thus, we obtain:

$$AT^2 + 2T - 2\Phi = 0 \tag{6}$$

where

$$A = \frac{-2T + 2\Phi}{T^2}, \quad T(x,t) \neq 0, \tag{7}$$

it is observed that the restriction $T(x,t) \neq 0$ in Eq. (7) is naturally satisfied when the thermal profile is measured in Kelvin. Thus, the constant A of $k(T)$ can be easily determined. Considering the case where the function $k(T)$ is given by the specific form $k(T) = k_0(A + BT)$, where A and B are constants, we have:

$$\Phi(x,t) = k(T) = \frac{1}{k_0}\int_0^T k_0(A + B\widehat{T})d\widehat{T} \Rightarrow AT + \frac{BT^2}{2} \tag{8}$$

Implying:

$$AT + \frac{BT^2}{2} = \Phi \tag{9}$$

Note that, in this case, it is not possible to isolate the constants A or B in Eq. (9) because they are linearly dependent. However, since the functions $T(x,t)$ and $\Phi(x,t)$ are known, the following linear system can be written:

$$\begin{cases} AT(x,t_1) + \frac{B}{2}T(x,t_1)^2 = \Phi(x,t_1) \\ AT(x,t_2) + \frac{B}{2}T(x,t_2)^2 = \Phi(x,t_2) \end{cases} \tag{10}$$

In the linear system, Eq.(10), the first equation is related to time $t = 1$ and the second to time $t = 2$. Thus, current temperatures are related to future temperatures, where $dt = t_2 - t_1$. The linear system can then be rewritten in matrix form:

$$\begin{bmatrix} A & B \end{bmatrix} \begin{bmatrix} T(x,t_1) & T(x,t_2) \\ \frac{T(x,t_1)^2}{2} & \frac{T(x,t_2)^2}{2} \end{bmatrix} = \begin{bmatrix} \Phi(x,t_1) & \Phi(x,t_2) \end{bmatrix} \tag{11}$$

It can be observed that the matrix containing the constants to be determined can be isolated in the matrix equation $TX = \Phi$, where the matrix X is represented by the set of coefficients A_n. Thus:

$$\begin{bmatrix} A & B \end{bmatrix} = \begin{bmatrix} \Phi(x,t_1) & \Phi(x,t_2) \end{bmatrix} \begin{bmatrix} T(x,t_1) & T(x,t_2) \\ \frac{T(x,t_1)^2}{2} & \frac{T(x,t_2)^2}{2} \end{bmatrix}^{-1} \tag{12}$$

Without loss of generality, we can consider the general case $k(T) = k_0(A_1 + A_2T + A_3T^2 + \cdots A_nT^{n-1})$. The dimension of the matrix containing the experimental and

linear temperatures depends on the number of constants to be determined. Therefore, as previously seen for the estimation of two coefficients, a square matrix of order 2 was obtained; it can be stated that if the model for the temperature-dependent thermal conductivity is a polynomial of the type $k(T)$ dependent on A_1, A_2, $\cdots$, A_n, it must have dimensions $n \times n$. Thus, starting from the matrix given by Eq.(12) and considering the estimation of n constants, we have, in general terms:

$$\mathbf{A} = \mathbf{\Phi}\,\mathbf{M}^{-1} \tag{13}$$

where $\mathbf{A} = [A_1, A_2, \ldots, A_n]$, $\mathbf{\Phi} = [\Phi(x,t_1), \Phi(x,t_2), \ldots, \Phi(x,t_n)]$, and $\mathbf{M}$ is the matrix:

$$\mathbf{M} = \begin{bmatrix} T(x,t_1) & T(x,t_2) & \cdots & T(x,t_n) \\ \frac{T(x,t_1)^2}{2} & \frac{T(x,t_2)^2}{2} & \cdots & \frac{T(x,t_n)^2}{2} \\ \vdots & \vdots & \ddots & \vdots \\ \frac{T(x,t_1)^n}{n} & \frac{T(x,t_2)^n}{n} & \cdots & \frac{T(x,t_n)^n}{n} \end{bmatrix} \tag{14}$$

Thus, Eq.(13) is the generalized form of the matrix in Eq.(12), allowing for the estimation of $k(T)$ from polynomial constants. Note that the matrix defined by the terms of T consists of temperature powers $T^0, T^1, \cdots T^n$, making it similar to a Vandermonde matrix, and it can become ill-conditioned if the temperature values are close to each other. Another factor to consider is that the coefficients of this matrix can have significantly different orders of magnitude due to the temperature powers. This implies that the matrix inversion process can be unstable, introducing errors that may be detrimental to solving the inverse problem.

In this regard, the estimations will be performed using a local (sequential) approach, estimating the thermal conductivity coefficients for multiple small data windows along the time domain, and subsequently calculating the average of the computed A_n coefficients. For a polynomial of degree N, $N+1$ independent points are necessary and sufficient to uniquely determine the $N+1$ coefficients A_n (from A_0 to A_N). For each window j, a square linear system of dimension $(N+1) \times (N+1)$ is assembled. The linear system for iteration j is, therefore:

$$\mathbf{M}^{(j)}\mathbf{A}^{(j)} = \mathbf{\Phi}^{(j)} \tag{15}$$

The above procedure, Eq. (15), generates a vector of estimates $\mathbf{A}$ for each possible sliding window position. If the total number of data points is D, the final vector of estimated coefficients, $\bar{\mathbf{A}}$, is obtained by calculating the arithmetic mean of all calculated estimates:

$$\bar{A}_p = \frac{1}{D}\sum_{j=1}^{D} \hat{A}_p^{(j)} \tag{16}$$

Therefore, determining the constants A_n of the polynomial $k(T)$ requires temperature measurements at an access point and temperatures calculated using the material's constant reference thermal conductivity, at the same point where the experimental

temperatures were measured. The following section describes the experimental procedure for obtaining the temperatures that will be used to apply the method proposed in this work.

3 Results and Discussion

3.1 Experimental Procedure

The experiment was conducted on a Romi CNC lathe available at LEPU/UFU through twenty tests using a tungsten carbide tool. Cast iron was selected as the workpiece material for its versatility. The workpieces were prepared as discs with axial channels, as shown in Fig. (1). A total of 20 tests were conducted, with each disc machined only once per day to ensure that thermal inertia did not affect the process's thermal behavior. Three type K thermocouples (AWG 36, 1000 ± 0.8 mm in length) were attached to the tool surface Fig. (2) using a capacitive discharge near the contact area with the workpiece. Their positions are listed in Tab. (2) (see Fig. (2)). The thermocouples were connected to a data acquisition system to record temperature signals during machining; the signals were acquired using a Keysight LXI Data Acquisition/Switch Unit during the machining process. Fig. (2) presents the complete assembly, including the instrumented tool and tool holder. Machining parameters, namely cutting speed, feed rate, spindle speed, and depth of cut, were kept constant, as listed in Tab. (1).

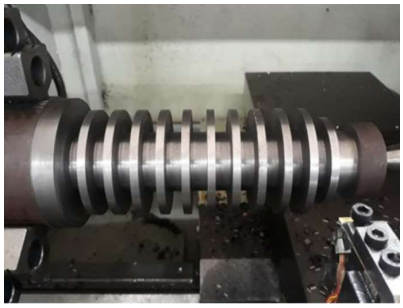

Fig. 1 Cast iron sample being machined [23].

Table 1 Machining parameters used in the tests [23].

Machining Parameters	**With Coating**	**Without Coating**
Cutting speed (v_c)	140 m/min	140 m/min
Feed rate (f)	0.12 mm/rev	0.12 mm/rev
Depth of cut (a_p)	13 mm	13 mm
Initial diameter	72 mm	54 mm
Final diameter	59 mm	41 mm
Disk thickness	5 mm	5 mm

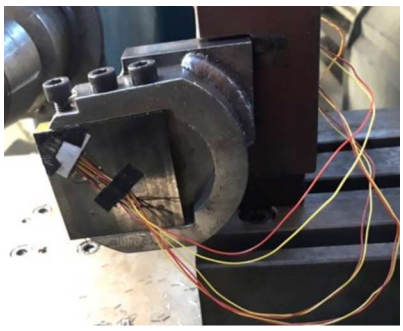

Fig. 2 Complete assembly showing the cutting tool and tool holder instrumented with thermocouples [23].

Tab. (2) presents the coordinates of the thermocouple where the temperatures were used for the development of this work, resulting in a thermal profile derived from the average temperature of the performed tests.

Table 2 Location for the tests, defined according to the coordinate axes [23].

Location	x [mm]	y [mm]	z [mm]
T3	1.72	10	1.95

3.2 Linear numerical solution of the thermal problem

As previously stated, the proposed method is computed using the experimental temperatures and the temperatures from the linear version of the thermal problem, using a reference thermal conductivity k_0. To obtain the linear solution of the problem, numerical methods based on finite elements and the ANSYS software are used. Fig. (3) shows the grid mesh; the three-dimensional modeling of the tool and tool holder assembly was carried out by CAD drawing using Siemens NX software, followed by importation into Ansys Fluent for the thermal solution. The mesh has $122,510$ nodes and $679,629$ elements with a size of 2.0×10^{-3} and a refinement of 5.0×10^{-4}. Table (3) presents the thermal properties of the materials involved in the model: tungsten carbide (WC-Co) insert and AISI 1045 carbon steel for the toolholder material. The thermal property values used for the tungsten carbide insert were obtained from [24], with the sample being the same insert used in this study. The solution of the linear problem can be obtained based on the previous heat flux estimation values by [23] and is presented in Fig. (5). The estimated heat flux was imposed on the tool-workpiece contact region Fig. (4), along with the heat transfer coefficient, which was applied uniformly to all exposed surfaces.

Table 3 Thermal properties of the materials used in the thermal model [24]

Parameters	Tungsten Carbide (WC-Co)	Toolholder (AISI 1045)
$\alpha\ [m^2/s]$	2.65×10^{-5}	4.5×10^{-6}
$k\ [W/mK]$	121.7	45

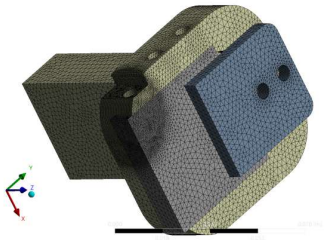

Fig. 3 Mesh used to FEM calculation [23].

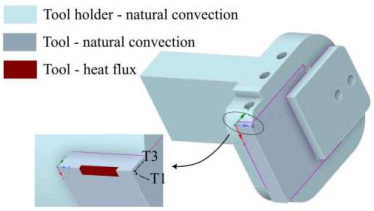

Fig. 4 Boundary conditions applied to FEM solver [23].

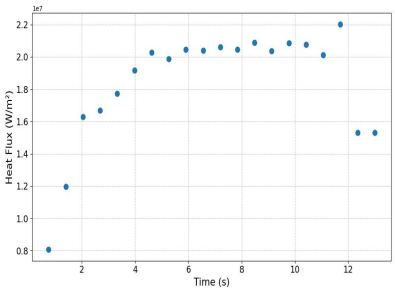

Fig. 5 Heat flux applied to FEM simulation [23].

Thus, the linear solution of the problem was calculated using the same experimental time range, except for a temporal discretization of $0.5s$, and at the exact T3 coordinates used for acquiring the experimental temperatures. Fig. (6) presents

the experimental temperatures and the temperatures calculated via finite element method (FEM) for the linear version of the problem. The experimental temperatures were resampled so that the linear and experimental vectors have the same dimension, ensuring the inverse problem matrices are constructed in the correct order. The resampling process was performed using linear interpolation through the `np.interp()` function from the Python NumPy library. Fig. (7) presents the resampled temperatures compared to the original experimental temperatures.

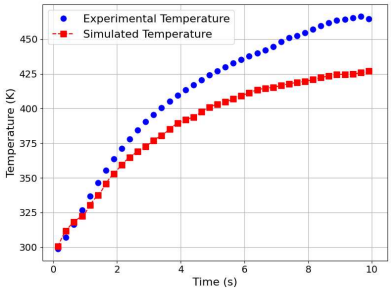

Fig. 6 Experimental and linear simulated temperature profiles for T3 coordinate.

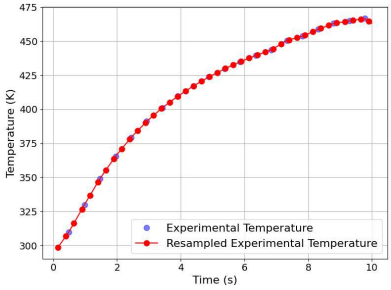

Fig. 7 Resampled experimental temperatures.

3.3 Inverse Problem Approach

Based on the resampled nonlinear experimental temperatures and the calculated linear temperatures Figs. (6, 7), we applied the proposed methodology for the case of a linear variation of the temperature-dependent thermal conductivity, $k(T) = k_0(A + BT)$. For this case, coefficients A and B were calculated using 17 square 2×2 linear systems within the time window framework, and ultimately an average value was calculated, as presented in Figs. (8, 9). Thus, for this case, the temperature-dependent thermal conductivity was estimated as:

$$k(T) = 121.7(1.1868 - 1.1703 \times 10^{-3}T) \tag{17}$$

Graphically, the thermal conductivity for the case $k(T) = k_0(A + BT)$, Eq. (17), is shown in Fig. (10). A decreasing behavior of thermal conductivity with increasing temperature can be observed, showing a 23.46% variation from $101 - 78$ W/mK. Due to the lack of knowledge regarding the actual behavior of the temperature-dependent thermal conductivity, a direct comparison is impossible. Therefore, the temperatures were recalculated via Ansys Fluent using the estimated parameters as the thermal conductivity input to observe whether the numerical model could recover the same experimental thermal profile, thus enabling a validation of the technique. Fig. (11) presents the comparison between the experimental and recalculated temperatures. We can observe that the recalculated temperatures are significantly close to the experimental temperatures, presenting relative errors of less than 2% Fig. (12).

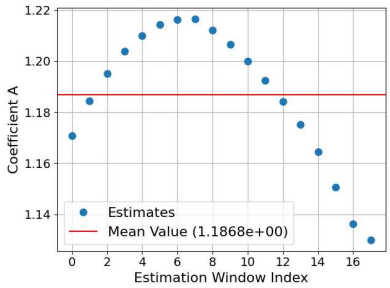

Fig. 8 The coefficient A estimated for each linear system and the mean value.

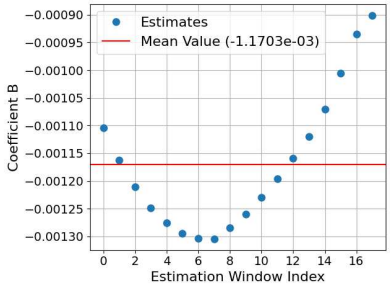

Fig. 9 The coefficient B estimated for each linear system and the mean value.

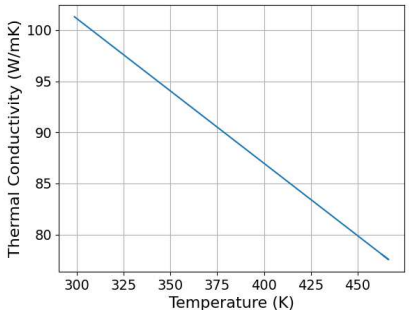

Fig. 10 Estimated temperature dependent thermal conductivity results by $k(T) = k_0(A + BT)$ application

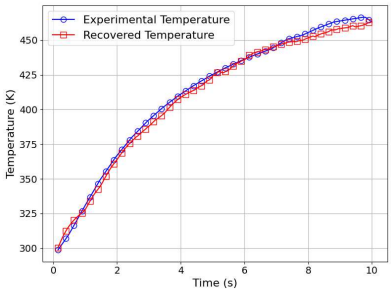

Fig. 11 Temperature comparison between experimental temperatures and numerical Ansys recovered temperatures using estimated $k(T) = k_0(A + BT)$

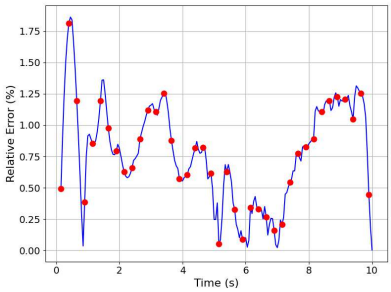

Fig. 12 Relative difference between experimental and recovered temperatures.

Similarly, the method was used to calculate the coefficients for a second-order polynomial thermal conductivity, $k(T) = k_0(A + BT + CT^2)$. The coefficients A, B, and C were calculated by assembling and solving 3×3 square linear systems for each of the 18 calculation time windows (Figs. 13, 14, and 15). Eq. (18) presents the

polynomial form for the estimated thermal conductivity, showing a 41.35% variation between the maximum and minimum values of $110.86 - 66.27$ W/mK. This behavior can be observed in Fig. (16).

$$k(T) = 121(0.9631 + 0.0011T - 4.5008 \times 10^{-6}T^2) \tag{18}$$

Constants A, B, and C are then applied to reconstruct the nonlinear temperatures, which were compared with the experimental temperatures Fig. (17). An excellent fit was observed in recovering the temperatures, with the relative error between the two profiles being less than 3.5%.

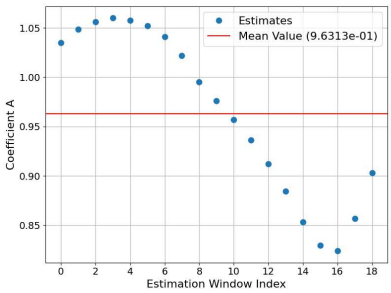

Fig. 13 The coefficient A estimated for each linear system and the mean value.

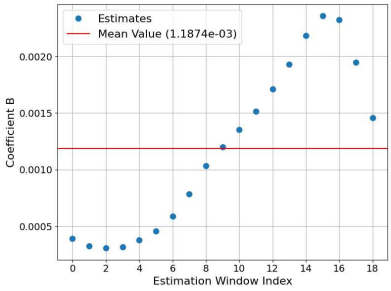

Fig. 14 The coefficient B estimated for each linear system and the mean value.

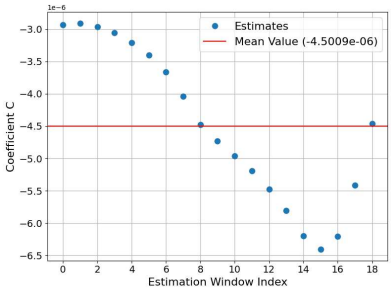

Fig. 15 The coefficient C estimated for each linear system and the mean value.

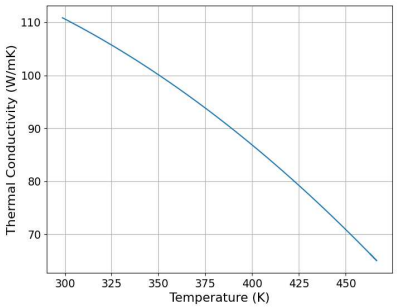

Fig. 16 Estimated temperature dependent thermal conductivity results by $k(T) = k_0(A+BT+CT^2)$ application.

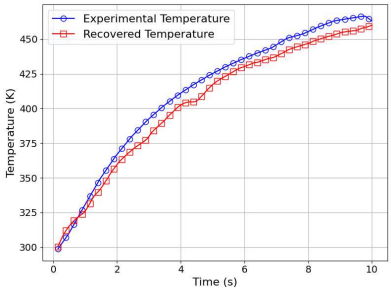

Fig. 17 Temperature comparison between experimental temperatures and numerical Ansys recovered temperatures using estimated $k(T) = k_0(A + BT + CT^2)$

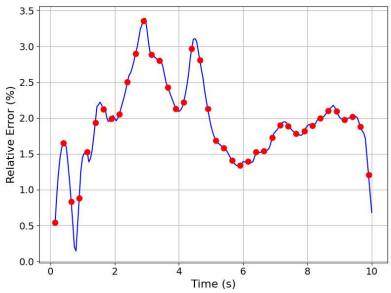

Fig. 18 Relative difference between experimental and recovered temperatures.

4 Conclusion

The estimation of temperature-dependent thermal conductivity proved to be a robust tool for determining the coefficients of $k(T)$ and reconstructing the experimental temperatures. It was observed that the estimation requires only knowledge of the experimental nonlinear temperatures, the linear thermal profile, and the reference thermal conductivity k_0, which can easily be obtained from the literature. The temperatures used in the estimations are derived from a single point on the access surface of the geometry, thus facilitating its application in experimental procedures.

Another fact to note is that the estimated constants are dependent on the sampled temperature variation; therefore, for each ΔT, there will be new values for the coefficients A_n. Observing the percentage differences between the experimental temperatures and those recalculated using the estimated coefficients reveals a strong approximation, with differences of less than 2% and 3.5% for the first- and second-order cases, respectively, thereby validating the development and application of the proposed technique.

Acknowledgements. The authors of this work would like to thank José Ricardo Ferreira Oliveira, José de Aguiar dos Santos Jr, and Vitor Oliveira for providing the experimental temperature data published in the work [23]. Furthermore, the authors acknowledge the financial support for the development of this research provided by: Fundação de Amparo à Pesquisa do Estado de Minas Gerais (FAPEMIG), Fundação Coordenação de Aperfeiçoamento de Pessoal de Nível Superior (CAPES), and Conselho Nacional de Desenvolvimento Científico e Tecnológico (CNPq).

References

[1] Veiga, F., Arizmendi, M., Jimenez, A., Gil Del Val, A.: Analytical thermal model of orthogonal cutting process for predicting the temperature of the cutting tool with temperature-dependent thermal conductivity. International Journal of Mechanical Sciences **204**, 106524 (2021) https://doi.org/10.1016/j.ijmecsci.2021.106524

[2] Zhao, J., Liu, Z., Wang, Q., Jiang, J.: Measurement of temperature-dependent thermal conductivity for PVD Ti0.55Al0.45N ceramic coating by time domain thermo-reflectance method. Ceramics International **45**, 8123–8129 (2019)

[3] Wang, X.M., Zhang, L.S., Yang, C., Liu, N., Cheng, W.L.: Estimation of temperature-dependent thermal conductivity and specific heat capacity for charring ablators. International Journal of Heat and Mass Transfer **129**, 894–902 (2019) https://doi.org/10.1016/j.ijheatmasstransfer.2018.10.014

[4] Tahmasbi, V., Noori, S.: Inverse identification of temperature-dependent thermal conductivity coefficients in an orthotropic charring composite. Applied Thermal Engineering **183**, 116219 (2021)

[5] Zhou, T., Xiao, H., Rao, Z.: Inverse method for simultaneously estimating temperature-dependent solid- and liquid-phase thermal conductivities during phase transition. International Communications in Heat and Mass Transfer **137**, 106220 (2022) https://doi.org/10.1016/j.icheatmasstransfer.2022.106220

[6] Cui, M., Zhao, Y., Xu, B.B., Wang, S., Gao, X.W.: Inverse analysis for simultaneously estimating multi-parameters of temperature-dependent thermal conductivities of an Inconel in a reusable metallic thermal protection system. Applied Thermal Engineering **125**, 480–488 (2017) https://doi.org/10.1016/j.applthermaleng.2017.06.113

[7] Yang, C.Y.: A linear inverse model for the temperature-dependent thermal conductivity determination in one-dimensional problems. Applied Mathematical Modelling **22**, 1–9 (1998)

[8] Yang, C.Y.: Estimation of the temperature-dependent thermal conductivity in inverse heat conduction problems. Applied Mathematical Modelling **23**, 469–478 (1999)

[9] Sawaf, B., Ozisik, M.N., Jarny, Y.: An inverse analysis to estimate linearly temperature dependent thermal conductivity components and heat capacity of an orthotropic medium. International Journal of Heat and Mass Transfer **38**(16), 3005–3010 (1995) https://doi.org/10.1016/0017-9310(95)00044-A

[10] Ribeiro, S.S.: Uso da Transformada de Kirchhoff e Funções de Green Para Solução Analítica de Problemas Inversos Não Lineares em Condução de Calor. Ph.D. thesis, Universidade Federal de Uberlândia (2019)

[11] Nigri, M.R., Pedrosa-Filho, J.J., Gama, R.M.S.: An exact solution for the heat transfer process in infinite cylindrical fins with any temperature-dependent thermal conductivity. Thermal Science and Engineering Progress **32**, 101333 (2022) https://doi.org/10.1016/j.tsep.2022.101333

[12] Yu, J., He, Y., Su, J.: Transient nonlinear heat conduction in a single-layer

pipe with temperature-dependent thermal conductivity: Integral transform and lumped model solutions. International Journal of Thermal Sciences **219**, 110258 (2026) https://doi.org/10.1016/j.ijthermalsci.2025.110258

[13] Farahani, S.D., Kisomi, M.S.: Experimental estimation of temperature-dependent thermal conductivity coefficient by using inverse method and remote boundary condition. International Communications in Heat and Mass Transfer **117**, 104736 (2020)

[14] Zhang, H., *et al.*: Measurement and identification of temperature-dependent thermal conductivity of thermal insulation materials under large temperature difference. International Journal of Thermal Sciences **171**, 107261 (2022) https://doi.org/10.1016/j.ijthermalsci.2021.107261

[15] Wang, F., Wang, Y., Sun, C., Zhang, P., Xia, X.: Experimental investigation on temperature-dependent effective thermal conductivity of ceramic fiber felt. International Journal of Thermal Sciences **200**, 108965 (2024) https://doi.org/10.1016/j.ijthermalsci.2024.108965

[16] Ramos, N.P., Antunes, M.M., Guimaraes, G., Silva, S.M.M.L.: Simultaneous Bayesian estimation of the temperature-dependent thermal properties of a metal slab using a three-dimensional transient experimental approach. International Journal of Thermal Sciences **179**, 107671 (2022) https://doi.org/10.1016/j.ijthermalsci.2022.107671

[17] Zheng, J., Huang, J., Huang, H.: Adaptive physics-informed neural network to simultaneously identify the temperature-dependent thermal conductivity and specific heat capacity of charring materials in hypersonic vehicle. Thermal Science and Engineering Progress **68**, 104408 (2025) https://doi.org/10.1016/j.tsep.2025.104408

[18] Qiu, W., Chen, H., Zhou, H.: A novel hybrid deep learning algorithm for estimating temperature-dependent thermal conductivity. International Communications in Heat and Mass Transfer **164**, 108871 (2025) https://doi.org/10.1016/j.icheatmasstransfer.2025.108871

[19] Zhang, L., Wang, J., Wu, L., Zhao, Y., Liu, Y., Huang, M., Chen, Z., Zhu, G., Zeng, X.: Temperature-dependent thermal conductivity and microscopic mechanisms in a Mg-Al-Y alloy. Journal of Rare Earths (2025) https://doi.org/10.1016/j.jre.2025.08.014 . In press

[20] Kim, M., Kim, D.M., Kim, Y.B., Lee, B.J.: Measurement of the temperature-dependent cross-plane thermal conductivity of the Li-ion battery pouch cell. Journal of Power Sources Advances **31**, 100167 (2025)

[21] Zhou, Y., Hu, X.X.: Two methods for estimation of temperature-dependent thermal conductivity based on constant element approximation. International Journal

of Thermal Sciences **135**, 104–116 (2019) https://doi.org/10.1016/j.ijthermalsci.2018.09.008

[22] Carslaw, H.S., Jaeger, J.C.: Conduction of Heat in Solids, 2nd edn. Clarendon Press, Oxford (1959)

[23] Oliveira, V.H.M., Ribeiro, S.S., Oliveira, J.R.F., Santos Jr, J.A., Silva, M.B., Guimaraes, G.: Comparative thermal analysis of TiN-coated and uncoated carbide cutting tools. The International Journal of Advanced Manufacturing Technology (2026) https://doi.org/10.1007/s00170-026-17558-z

[24] Aguiar, J., Ferreira-Oliveira, J.R., Riffel, D.B., Guimaraes, G.: Analysis of the effect of surface coating and texturization on the estimation of effective thermophysical properties. Thermal Science and Engineering Progress **50**, 102558 (2024) https://doi.org/10.1016/j.tsep.2024.102558